 doi:10.20944/preprints201806.0111.v1

Article

A Five-bar Planar Parallel Manipulator with two End-effectors

Jaime Gallardo-Alvarado*, Ramon Rodriguez-Castro, Luciano Perez-Gonzalez, Carlos R. Aguilar-Najera and Alvaro Sanchez-Rodriguez

Department of Mechanical Engineering, Instituto Tecnologico de Celaya, TecNM, Av. Tecnologico y A Garcia Cubas, 38010 Celaya, Gto, Mexico

* jaime.gallardo@itcelaya.edu.mx, tel: +52 461 61 1 75 75, fax: +52 461 61 1 79 79.

Abstract: Parallel manipulators with multiple end-effectors bring us interesting advantages over conventional parallel manipulators such as improved manipulability, workspace and avoidance of singularities. In this work the kinematics of a five-bar planar parallel manipulator equipped with two end-effectors is approached by means of the theory of screws. As an intermediate step the displacement analysis of the robot is also investigated. The input-output equations of velocity and acceleration are systematically obtained by resorting to reciprocal-screw theory. In that regard the Klein form of the Lie algebra $se(3)$ of the Euclidean group $SE(3)$ plays a central role. In order to exemplify the method of kinematic analysis, a case study is included. Furthermore, the numerical results obtained by means of the theory of screws are confirmed with the aid of special software like ADAMS.TM

Keywords: parallel manipulator; multiple end-effectors; Klein form; screw theory; kinematics

1. Introduction

The benefits and drawbacks of serial and parallel manipulators have been widely discussed in the literature, as a result of this productive exchange of ideas and knowledge, mainly emerging from the kinematician community, academia and industry have been generously benefited with the introduction of creative and ingenious robots able to operate under conditions demanding flexibility as well as high precision and dynamic performance; characteristics that exceed definitively the human capacity.

Despite the effervescent success of modern robotics and its positive impact on the industrial environment and in the society in general, the improvement of existing mathematical methods of analysis and the proposal of new topologies still being the inspiration for many kinematicians. In that concern, with the purpose to improve the dexterity and workspace of parallel manipulators, keeping their benefits like rigidity and precision, recently robot manipulators with multiple end-effectors and reconfigurable platforms have been introduced [1]. In this work the kinematics of a redundant planar manipulator with multiple end-effectors is investigated by means of the theory of screws. The base mechanism of the proposed robot is the typical five-bar planar parallel manipulator.

Eventhough its simplicity, the five-bar planar parallel manipulator, 5R mechanism for brevity, has been extensively studied approaching issues like inverse-forward kinematics, singularity analysis, optimal workspace, kinematic calibration, topology optimization, robot performance and so on, see for instance [2–7]. On the other hand as occur for most parallel manipulators, limited workspace is a drawback of the 5R mechanism, e.g. Briot and Goldsztejn [7] proposed a regular dextrous workspace of an optimized 5R mechanism as the area of a rectangle delimited by the workspace boundary and the direct singularities. In that regard the workspace of a 2R open kinematic chain is the area delimited by two concentric circles whose radii depend on the extreme condition folded/unfolded of the serial kinematic chain. Furthermore, arbitrary poses of a rigid body are not available for the 5R mechanism. However the benefits of the 5R mechanism are indisputable, e.g., it was applied in the development of the MELFA RP Series robots in the Mitsubishi Electric Corporation. Therefore it is worth to develop

Preprints (www.preprints.org) | NOT PEER-REVIEWED | Posted: 7 June 2018 doi:10.20944/preprints201806.0111.v1

robot manipulators based on the topology of the 5R mechanism alleviating its drawbacks incorporating additional kinematic elements.

In this work two 2R serial kinematic chains working as two end-effectors are assembled to the upper links of the 5R mechanism yielding a hybrid robot manipulator (HRM). For simplicity, the 5R mechanism is chosen as a symmetric planar parallel manipulator. The rest of the contribution is organized as follows. In section 2 the HRM and its geometry is briefly described. The displacement analysis is presented in section 3 for the sake of completeness. The inverse-forward displacement analysis is easily approached based on simple closure equations The instantaneous kinematics, up to the acceleration analysis, is approached in section 4. With the purpose to exemplify the method in section 5 a case study is provided. Finally, some conclusions are given at the end of the contribution.

2. Description of the Robot Manipulator

Figure 1 shows how the concepts of configurable platform and multiple end-effectors can improve considerably the capacity of a simple closed kinematic chain yielding, in this case, a hybrid robot manipulator (HRM), e.g., the end-effectors of the HRM would work together as two cooperating manipulators in addition to the typical operations of serial and parallel manipulators. The idea is simple but effective. Firstly, the four-bar mechanism is considered as a parallel manipulator where the coupler link is chosen as the moving platform. Secondly, the moving platform is transformed into a configurable platform formed with four articulated bars. Finally, two of the articulated links of the configurable platform are removed, a practical decision, and one 2R open kinematic chain playing the role of end-effector is attached to each one of the remaining links of the configurable platform.

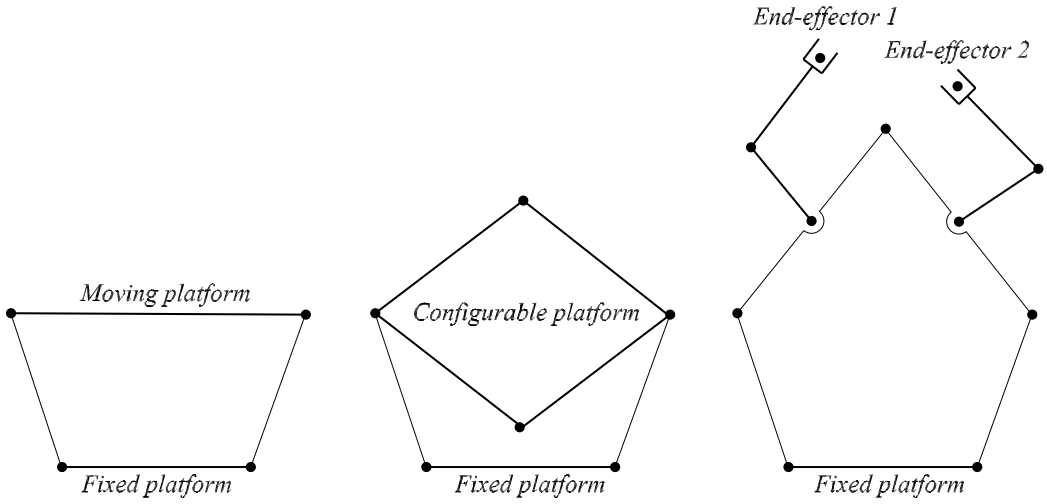

Figure 1. Transition of a closed kinematic chain into a hybrid robot manipulator

Hence, the proposed robot manipulator, right planar mechanism of Fig. 2, consists of two end-effectors sharing a five-bar planar mechanism. The five-bar mechanism is a planar parallel mechanism which owing its two degrees of freedom is used for positioning a point on a region of the workspace. The five bars are serially connected by means of revolute joints where conveniently the two revolute joints mounted on the base link are actuated.

In order to explain the geometry of the HRM let us consider that XY is a reference frame attached to the base link whose origin is located at point O_1, see Fig. 2. Afterwards, let us consider that h denotes the length of the base link while the lengths of the lower and upper links of the legs of the 5R mechanism are denoted, respectively, by a and b. The orientation of the lower links is controlled by means of the lower generalized coordinates $\underline{q}_i$ which are characterized by points O_i located by vectors

Preprints (www.preprints.org) | NOT PEER-REVIEWED | Posted: 7 June 2018 doi:10.20944/preprints201806.0111.v1

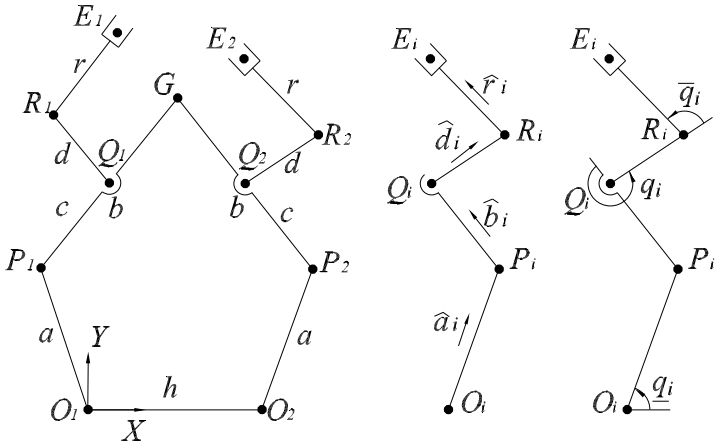

Figure 2. Geometry scheme of the hybrid robot manipulator

$\boldsymbol{o}_i$. Unless otherwise, in the rest of the paper $i = 1, 2$. The end of the lower links are denoted by points P_i located by vectors $\boldsymbol{p}_i$. The output point of the 5R mechanism is the point G which is located by vector $\boldsymbol{g}$ and of course also is the common point of the two legs of the 5R mechanism. The ith 2R serial chain is connected to the 5R mechanism through a revolute joint denoted by point Q_i, located by vector $\boldsymbol{q}_i$, in which c denotes the distance between points P_i and Q_i. The arm and forearm of the ith end effector are denoted by the lengths d and r and are articulated by means of a revolute joint characterized by point R_i, located by vector $\boldsymbol{r}_i$. Naturally, the revolute joints of the end-effectors are actuated according to the middle and upper generalized coordinates q_i and $\bar{q}_i$. Thus the set of generalized coordinates are notated as $\{\underline{q}_i, q_i, \bar{q}_i\}$. Finally, the positions of the end-effectors are denoted by points E_i, located by vectors $\boldsymbol{e}_i$. With the purpose to arrive at point E_i, beginning from point O_i, let us consider four unit vectors: i) $\hat{\boldsymbol{a}}_i$ expresses a unit vector pointed from O_i to P_i, ii) $\hat{\boldsymbol{b}}_i$ denotes a unit vector directed from P_i to Q_i, iii) $\hat{\boldsymbol{d}}_i$ stands for a unit vector pointed from Q_i to R_i and, iv) $\hat{\boldsymbol{r}}_i$ is a unit vector specified from R_i to E_i.

3. Displacement analysis

In this section the finite kinematics of the HRM manipulator is presented.

3.1. Displacement Analysis of the 5R Mechanism

3.1.1. Forward Displacement Analysis of the 5R Mechanism

The forward displacement analysis consists of finding the coordinates of the output point $G = (X_G, Y_G)$ given the lower generalized coordinates $\underline{q}_i$. Since G is described by the vector $\boldsymbol{g}$ then the analysis may be solved based on the following two closure equations

$$(\boldsymbol{g} - \boldsymbol{p}_i) \cdot (\boldsymbol{g} - \boldsymbol{p}_i) = b^2 \tag{1}$$

in which $\boldsymbol{p}_i = \boldsymbol{o}_i + a\hat{\boldsymbol{a}}_i$ where $\hat{\boldsymbol{a}}_i = \cos\underline{q}_i\hat{\boldsymbol{i}} + \sin\underline{q}_i\hat{\boldsymbol{j}}$. Meanwhile the dot $(\cdot)$ denotes the inner product of three-dimensional vector algebra. From expressions (1) one obtains two quadratic equations in the unknown coordinates X_G and Y_G which may be reduced after a few computations into two simple equations as follows

$$(1 + K_1^2)X_G^2 + 2(K_1K_2 - a\cos\underline{q}_1 - K_1 a\sin\underline{q}_1)X_G + a^2 - b^2 + K_2^2 - 2K_2 a\sin\underline{q}_1 = 0, Y_G = K_1X_G + K_2 \tag{2}$$

where the coefficients K_1 and K_2 are given by

Preprints (www.preprints.org) | NOT PEER-REVIEWED | Posted: 7 June 2018 doi:10.20944/preprints201806.0111.v1

$K_1 = (a\cos\underline{q}_1 - a\cos\underline{q}_2 - h)/a(\sin\underline{q}_2 - \sin\underline{q}_1)$
$K_2 = (ha\cos\underline{q}_2 + h^2/2)/a(\sin\underline{q}_2 - \sin\underline{q}_1)$

As it was expected, given the parameters of the 5R mechanism and the lower generalized coordinates $\underline{q}_1$ and $\underline{q}_2$, the output point G can reach at most two positions.

3.1.2. Inverse Displacement Analysis of the 5R Mechanism

The inverse displacement analysis of the 5R mechanism consists of finding their configurations given the coordinates of point G, e.g., it is required to compute the lower generalized coordinates $\underline{q}_i$ given the coordinates of point G. To this end from Eq. (1) an expression of the form

$$A_i \sin(\underline{q}_i) + B_i \cos(\underline{q}_i) = C_i \tag{3}$$

is easily derived in which the coefficients are given by

$A_i = 2aY_G$,
$B_i = 2aX_G - 2\delta_i ah$ where $\delta_1 = 0$, $\delta_2 = 1$,
$C_i = X_G^2 + Y_G^2 + a^2 - b^2 + \delta_i h^2$

Equation (3) yields a quadratic equation in the unknown $\sin\underline{q}_i$ as follows

$$(A_i^2 + B_i^2)\sin^2\underline{q}_i - 2A_iC_i\sin\underline{q}_i + C_i^2 - B_i^2 = 0 \tag{4}$$

Therefore there are four possible solutions for the inverse displacement analysis of the 5R mechanism.

3.2. *Displacement Analysis of the Open Kinematic Chains*

In order to approach the displacement analysis of the two open kinematic chains let us consider that the position vector $\boldsymbol{e}_i$ of E_i may be obtained as

$$\boldsymbol{e}_i = \boldsymbol{o}_i + a\hat{\boldsymbol{a}}_i + c\hat{\boldsymbol{b}}_i + d\hat{\boldsymbol{d}}_i + r\hat{\boldsymbol{r}}_i \tag{5}$$

Therein, the unit vectors $\hat{\boldsymbol{d}}_i$ and $\hat{\boldsymbol{r}}_i$ may be obtained as $\hat{\boldsymbol{d}}_i = \mathrm{R}_{qi}\hat{\boldsymbol{b}}_i$ and $\hat{\boldsymbol{r}}_i = \mathrm{R}_{\bar{q}i}\hat{\boldsymbol{d}}_i$ where R_{qi} and $\mathrm{R}_{\bar{q}i}$ are the usual rotation matrices built according to the middle and upper generalized coordinates q_i and $\bar{q}_i$, respectively. Meanwhile, it is evident that $\hat{\boldsymbol{b}}_i = (\boldsymbol{g} - \boldsymbol{p}_i)/b$.

3.2.1. Forward Displacement Analysis of the Open Kinematic Chains

This analysis comprises the computation of the coordinates of points E_i for a set of generalized coordinates $\underline{q}_i$, q_i and $\bar{q}_i$. Once the forward displacement analysis of the 5R mechanism is solved, see subsection 3.1.1, the coordinates of E_i are obtained by a direct application of Eq. (5). Hence, each point E_i can reach at most two locations.

3.2.2. Inverse Displacement Analysis of the Open Kinematic Chains

This analysis deals with the computation of the generalized coordinates of the HRM given the coordinates of points E_i. The possibilities of this analysis are immense due to the inclusion of extra generalized coordinates. For example assuming values for the lower revolute joints, then the coordinates of points Q_i, which are located by vectors $\boldsymbol{q}_i$, may be resolved taking into account that $\boldsymbol{q}_i = \boldsymbol{o}_i + c\hat{\boldsymbol{b}}_i$. Afterwards, with the purpose to compute the generalized coordinates Q_i and R_i the following closure equations would be considered for each open chain

$$(\hat{\boldsymbol{e}}_i - \boldsymbol{r}_i)\cdot(\hat{\boldsymbol{e}}_i - \boldsymbol{r}_i) = e_i^2, \quad (\hat{\boldsymbol{r}}_i - \boldsymbol{o}_i - c\hat{\boldsymbol{b}}_i)\cdot(\hat{\boldsymbol{r}}_i - \boldsymbol{o}_i - c\hat{\boldsymbol{b}}_i) = r^2 \tag{6}$$

Following the method of the displacement analysis realized for the 5R mechanism, the position vectors $\boldsymbol{r}_i$ are determined solving Eqs. (6), and the computation of the generalized coordinates q_i and $\bar{q}_i$ is immediate.

Preprints (www.preprints.org) | NOT PEER-REVIEWED | Posted: 7 June 2018 doi:10.20944/preprints201806.0111.v1

4. Instantaneous Kinematics

In this section the velocity and acceleration analyses of the HRM are addressed by means of the theory of screws. The screws representing the revolute joints and reciprocal lines of the robot manipulator are shown in Fig. 3. For details of this section the reader is referred to Gallardo-Alvarado [8].

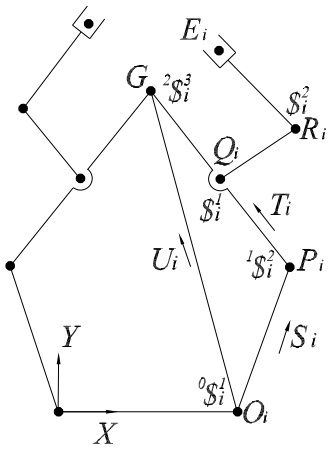

Figure 3. The screws of the hybrid robot manipulator

Let us consider that m is a rigid body in motion with respect to another body or reference frame labeled 0. Furthermore, let us consider that ${}^0\boldsymbol{\omega}^m$ is the angular velocity vector of m as measured from the reference frame 0 while $\boldsymbol{v}_*$ is the linear velocity vector of an arbitrary point $(*)$ of m. The vectors ${}^0\boldsymbol{\omega}^m$ and $\boldsymbol{v}_*$ form an inseparable entity named the velocity state of m with respect to 0, notated as ${}^0\boldsymbol{V}^m$. In fact, the velocity state of body m is defined as a six-dimensional vector ${}^0\boldsymbol{V}^m$ created with two concatenated vectors namely the primal and dual parts of the velocity state notated as $p({}^0\boldsymbol{V}^m)$ and $d({}^0\boldsymbol{V}^m)$, respectively. The first one is the vector ${}^0\boldsymbol{\omega}^m$ while the second one is the vector $\boldsymbol{v}_*$, i.e., ${}^0\boldsymbol{V}^m \equiv (p({}^0\boldsymbol{V}^m), d({}^0\boldsymbol{V}^m)) = ({}^0\boldsymbol{\omega}^m, \boldsymbol{v}_*)$. The confirmation of the equivalence of the velocity state of rigid body as a twist about a screw is one of the most relevant contributions of the theory of screws to the study of the kinematics of rigid body, specially in the field of robot kinematics, e.g., assuming that m is the end effector of an open kinematic chain while 0 is the base link then the velocity state of m as measured from 0 may be expressed as a linear combination of the infinitesimal screws representing the kinematic pairs of the open chain as follows

$$ {}^0\boldsymbol{V}^m = {}_0\omega_1\ {}^0\$^{1_O} + {}_1\omega_2\ {}^1\$^{2_O} + \ldots + {}_{m-2}\omega_{m-1}\ {}^{m-2}\$^{m-1_O} + {}_{m-1}\omega_m\ {}^{m-1}\$^{m_O} \tag{7} $$

where ${}_{k-1}\omega_k$ is the joint rate between the adjacent bodies $k-1$ and k while O is the reference point for computing the Plücker coordinates of the infinitesimal screws, also known as the reference pole. If the reference pole (O) is the point $(*)$ then ${}^0\boldsymbol{V}^m_* = {}^0\boldsymbol{V}^m$. Otherwise, according to the theory of helicoidal vector fields we have

$$ {}^0\boldsymbol{V}^m_* = \begin{bmatrix} p({}^0\boldsymbol{V}^m) \\ d({}^0\boldsymbol{V}^m) + p({}^0\boldsymbol{V}^m) \times \boldsymbol{r}_{*/O} \end{bmatrix} \tag{8} $$

where $\boldsymbol{r}_{*/O}$ is the position vector of $*$ with respect to O.

On the other hand, the reduced acceleration state, or accelerator for brevity, of rigid body m as observed from body 0 is defined as a six-dimensional vector ${}^0\boldsymbol{A}^m$ built with two concatenated vectors namely the primal and dual parts of the accelerator. The primal part corresponds to the angular acceleration vector ${}^0\boldsymbol{\alpha}^m$, i.e. ${}^0\boldsymbol{\alpha}^m = \frac{d}{dt}{}^0\boldsymbol{\omega}^m$, while the dual part is a composed vector given by $\boldsymbol{a}_* - {}^0\boldsymbol{\omega}^m \times \boldsymbol{v}_*$ in which $\boldsymbol{a}_*$ is the linear acceleration vector of point $(*)$, i.e. $\boldsymbol{a}_* = \frac{d}{dt}\boldsymbol{v}_*$. In fact, the

Preprints (www.preprints.org) | NOT PEER-REVIEWED | Posted: 7 June 2018 doi:10.20944/preprints201806.0111.v1

accelerator is defined as ${}^0\boldsymbol{A}^m \equiv (p({}^0\boldsymbol{A}^m), d({}^0\boldsymbol{A}^m)) = ({}^0\boldsymbol{\alpha}^m, \boldsymbol{a}_* - {}^0\boldsymbol{\omega}^m \times \boldsymbol{v}_*)$. Furthermore, in an open serial chain the accelerator may be written in screw form as follows

$$ {}^0\boldsymbol{A}^m = {}_0\alpha_1\, {}^0\$^{1_O} + {}_1\alpha_2\, {}^1\$^{2_O} + \ldots + {}_{m-2}\alpha_{m-1}\, {}^{m-2}\$^{m-1_O} + {}_{m-1}\alpha_m\, {}^{m-1}\$^{m_O} + {}^0\boldsymbol{L}^m \tag{9} $$

where ${}_{k-1}\alpha_k = \frac{d}{dt}{}_{k-1}\omega_k$. Meanwhile, ${}^0\boldsymbol{L}^m$ is the Lie screw of acceleration which is given by

$$ \begin{aligned} {}^0\boldsymbol{L}^m = & \begin{bmatrix} {}_0\omega_1\, {}^0\$^{1_O} & {}_1\omega_2\, {}^1\$^{2_O} + \ldots + {}_{m-2}\omega_{m-1}\, {}^{m-2}\$^{m-1_O} + {}_{m-1}\omega_m\, {}^{m-1}\$^{m_O} \end{bmatrix} \\ & + \begin{bmatrix} {}_1\omega_2\, {}^1\$^{2_O} & {}_2\omega_3\, {}^2\$^{3_O} + \ldots + {}_{m-2}\omega_{m-1}\, {}^{m-2}\$^{m-1_O} + {}_{m-1}\omega_m\, {}^{m-1}\$^{m_O} \end{bmatrix} \\ & + \ldots + \begin{bmatrix} {}_{m-2}\omega_{m-1} & {}^{m-2}\$^{m-1_O} + {}_{m-1}\omega_m\, {}^{m-1}\$^{m_O} \end{bmatrix} \end{aligned} \tag{10} $$

4.1. Instantaneous Kinematics of the 5R Mechanism

Let us consider that ${}^0\boldsymbol{V}_G^G = (\boldsymbol{\omega}, \boldsymbol{v}_G)$ is the velocity state of G as observed from the base link, where point G plays the role of reference pole. It is evident that due to the planar nature of the robot manipulator at hand some terms of the velocity state vanish, i.e., ${}^0\boldsymbol{V}_G^G = (\boldsymbol{\omega}, \boldsymbol{v}_G) = \begin{bmatrix} 0 & 0 & \omega_Z & v_{GX} & v_{GY} & 0 \end{bmatrix}^T$. On the other hand, the velocity state ${}^0\boldsymbol{V}_G^G$ may be written in screw form as follows

$$ {}^0\boldsymbol{V}_G^G = {}_0\omega_1^i\, {}^0\$_i^1 + {}_1\omega_2^i\, {}^1\$_i^2 + {}_2\omega_3^i\, {}^2\$_i^3 \tag{11} $$

where ${}_0\omega_1^i = \dot{\underline{q}}_i$ is the ith lower generalized velocity.

In order to obtain the linear input-output equation of velocity of the 5R mechanism let us consider that $\boldsymbol{T}_i$ is a line in Plücker coordinates directed from P_i to G, e.g. $\boldsymbol{T}_i = (\boldsymbol{b}_i, \boldsymbol{0})$ advised that G is the reference pole. The application of the Klein form of the line $\boldsymbol{T}_i$ to both sides of expression (11) with the reduction of terms leads to

$$ \{\boldsymbol{T}_i; {}^0\boldsymbol{V}_G^G\} = \dot{\underline{q}}_i \{\boldsymbol{T}_i; {}^0\$_i^1\} \tag{12} $$

Hence, after a few computations the linear input-output equation of velocity of the 5R mechanism results in

$$ \underline{\mathrm{J}}^T \begin{bmatrix} v_{GX} \\ v_{GY} \end{bmatrix} = \mathrm{J}\, \mathrm{Q}_v \tag{13} $$

where

$\underline{\mathrm{J}} = \begin{bmatrix} \hat{\boldsymbol{b}}_1 & \hat{\boldsymbol{b}}_2 \end{bmatrix}$ is the direct Jacobian matrix of the 5R mechanism,
$\mathrm{J} = \mathrm{diag} \begin{bmatrix} \{\boldsymbol{T}_1; {}^0\$_1^1\} & \{\boldsymbol{T}_2; {}^0\$_2^1\} \end{bmatrix}$ is the inverse Jacobian matrix of the 5R mechanism, and
$\mathrm{Q}_v = \begin{bmatrix} \dot{\underline{q}}_1 & \dot{\underline{q}}_2 \end{bmatrix}^T$ is the first-order driver matrix of the 5R mechanism.

In order to compute the passive joint velocity rates ${}_1\omega_2^i$ and ${}_2\omega_3^i$, a necessary step for approaching the acceleration analysis, let us consider two lines in Plücker coordinates for each leg of the 5R mechanism: i) $\boldsymbol{U}_i$ is a line pointed from O_i to G, i.e. $\boldsymbol{U}_i = (\hat{\boldsymbol{u}}_i, \boldsymbol{0})$ where $\hat{\boldsymbol{u}}_i = (\boldsymbol{g} - \boldsymbol{o}_i) / \mid \boldsymbol{g} - \boldsymbol{o}_i \mid$, ii) $\boldsymbol{S}_i$ is a line pointed from O_i to P_i, i.e. $\boldsymbol{S}_i = (\hat{\boldsymbol{a}}_i, \hat{\boldsymbol{a}}_i \times \boldsymbol{r}_{G/O_i})$. Thus by taking advantage of the concept of reciprocal screw it follows that

$$ {}_1\omega_2^i = \{\boldsymbol{U}_i; {}^0\boldsymbol{V}_G^G\} / \{\boldsymbol{U}_i; {}^1\$_i^2\}, \quad {}_2\omega_3^i = \{\boldsymbol{S}_i; {}^0\boldsymbol{V}_G^G\} / \{\boldsymbol{S}_i; {}^2\$_i^3\} \tag{14} $$

Finally, once the joint velocity rates ${}_1\omega_2^i$ and ${}_2\omega_3^i$ are computed, the angular velocity vector $\boldsymbol{\omega}$ is obtained as the primal part of ${}^0\boldsymbol{V}_G^G$ by resorting to Eqs. (11), (17) and (14).

In what follows the acceleration analysis of the 5R mechanism is presented. The reduced acceleration state of point G may be written as ${}^0\boldsymbol{A}_G^G = (\boldsymbol{\alpha}, \boldsymbol{a}_G - \boldsymbol{\omega} \times \boldsymbol{v}_G)$. However, it is evident that due to the planar nature of the robot manipulator at hand some terms of the accelerator vanish,

Preprints (www.preprints.org) | NOT PEER-REVIEWED | Posted: 7 June 2018 doi:10.20944/preprints201806.0111.v1

i.e., ${}^0\boldsymbol{A}_G^G = (\boldsymbol{\alpha}, \boldsymbol{a}_G - \boldsymbol{\omega} \times \boldsymbol{v}_G) = \begin{bmatrix} 0 & 0 & \alpha_Z & a_{GX} + \omega_Z v_{GY} & a_{GY} - w_Z v_{GX} & 0 \end{bmatrix}^T$. Furthermore, the accelerator ${}^0\boldsymbol{A}_G^G$ may be written in screw form as follows

$$ {}^0\boldsymbol{A}_G^G = {}_0\alpha_1^i \, {}^0\$_i^1 + {}_1\alpha_2^i \, {}^1\$_i^2 + {}_2\alpha_3^i \, {}^2\$_i^3 + {}^0\boldsymbol{L}_G^{Gi} \tag{15} $$

where ${}_0\alpha_1^i = \ddot{\underline{q}}_i$ is the ith lower generalized acceleration. Meanwhile, ${}^0\boldsymbol{L}_G^{Gi}$ is the ith Lie screw of acceleration which is calculated as follows

$$ {}^0\boldsymbol{L}_G^{Gi} = \begin{bmatrix} {}_0\omega_1^i \, {}^0\$_i^1 & {}_1\omega_2^i \, {}^1\$_i^2 + {}_2\omega_3^i \, {}^2\$_i^3 \end{bmatrix} + \begin{bmatrix} {}_1\omega_2^i \, {}^1\$_i^2 & {}_2\omega_3^i \, {}^2\$_i^3 \end{bmatrix} \tag{16} $$

where the brackets, $[* \quad *]$, denote the Lie product or outer product of the Lie algebra $se(3)$ of the Euclidean group $SE(3)$.

Following the trend of the velocity analysis, the linear input-output equation of acceleration of the 5R mechanism results in

$$ \underline{\mathrm{J}}^T \begin{bmatrix} a_{GX} + \omega_Z v_{GY} \\ a_{GY} - \omega_Z v_{GX} \end{bmatrix} = \mathrm{J}\, \mathrm{Q}_a + \begin{bmatrix} \{\boldsymbol{T}_1; \boldsymbol{L}_{G1}\} \\ \{\boldsymbol{T}_2; \boldsymbol{L}_{G2}\} \end{bmatrix} \tag{17} $$

where $\mathrm{Q}_a = \begin{bmatrix} \ddot{\underline{q}}_1 & \ddot{\underline{q}}_2 \end{bmatrix}^T$ is the second-order driver matrix of the 5R mechanism. Furthermore, the passive joint acceleration rates are given by

$$ {}_1\alpha_2^i = \{\boldsymbol{U}_i; {}^0\boldsymbol{A}_G^G - {}^0\boldsymbol{L}_G^{Gi}\} / \{\boldsymbol{U}_i; {}^1\$_i^2\}, \quad {}_2\omega_3^i = \{\boldsymbol{S}_i; {}^0\boldsymbol{A}_G^G - {}^0\boldsymbol{L}_G^{Gi}\} / \{\boldsymbol{S}_i; {}^2\$_i^3\} \tag{18} $$

4.2. Instantaneous Kinematics of the Open Chains

Once the passive joint velocity rate ${}_1\omega_2^i$ was computed, see Eq. (14), the velocity state of the ith end-effector may be determined as follows

$$ {}^0\boldsymbol{V}_G^{Ei} = \dot{\underline{q}}_i \, {}^0\$_i^1 + {}_1\omega_2^i \, {}^1\$_i^2 + \dot{q}_i \$_i^1 + \dot{\tilde{q}}_i \$_i^2 \tag{19} $$

Furthermore, according to the theory of helicoidal vector fields, the velocity state of the ith end-effector considering point E_i as the reference pole is given by

$$ {}^0\boldsymbol{V}_{Ei}^{Ei} = \begin{bmatrix} \boldsymbol{\omega}_{Ei} \\ \boldsymbol{v}_{Ei} \end{bmatrix} = \begin{bmatrix} p({}^0\boldsymbol{V}_G^{Ei}) \\ d({}^0\boldsymbol{V}_G^{Ei}) + p({}^0\boldsymbol{V}_G^{Ei}) \times \boldsymbol{r}_{E_i/G} \end{bmatrix} \tag{20} $$

where $\boldsymbol{r}_{E_i/G}$ is the position vector of E_i with respect to G. Meanwhile, $\boldsymbol{\omega}_{Ei}$ is the angular velocity vector of the ith end-effector whereas $\boldsymbol{v}_{Ei}$ is the velocity of point E_i. It is worth to note that according to Eq. (19) there is a unique solution for solving the forward velocity analysis given the joint velocity rates $\dot{\underline{q}}_i$, $\dot{q}_i$ and $\dot{\tilde{q}}_i$ whereas for the solution of the inverse velocity analysis there is an infinite of possibilities, e.g., given the velocity state ${}^0\boldsymbol{V}_{Ei}^{Ei}$ one can freely choose arbitrary lower generalized speeds $\dot{\underline{q}}_1$ and $\dot{\underline{q}}_2$ and then the computation of the required values of $\dot{q}_i$ and $\dot{\tilde{q}}_i$ is straightforward by resorting to Eq. (19).

With the purpose to approach the acceleration analysis let us consider that the accelerator of the ith end-effector may be written in screw form as follows

$$ {}^0\boldsymbol{A}_G^{Ei} = \ddot{\underline{q}}_i \, {}^0\$_i^1 + {}_1\alpha_2^i \, {}^1\$_i^2 + \ddot{q}_i \$_i^1 + \ddot{\tilde{q}}_i \$_i^2 + {}^0\boldsymbol{L}_G^{Ei} \tag{21} $$

where the ith Lie screw of acceleration ${}^0\boldsymbol{L}_G^{Ei}$ is computed as

$$ {}^0\boldsymbol{L}_G^{Ei} = \begin{bmatrix} \dot{\underline{q}}_i \, {}^0\$_i^1 & {}_1\omega_2^i \, {}^1\$_i^2 + \dot{q}_i \$_i^1 + \dot{\tilde{q}}_i \$_i^2 \end{bmatrix} + \begin{bmatrix} {}_1\omega_2^i \, {}^1\$_i^2 & \dot{q}_i \$_i^1 + \dot{\tilde{q}}_i \$_i^2 \end{bmatrix} + \begin{bmatrix} \dot{q}_i \$_i^1 & \dot{\tilde{q}}_i \$_i^2 \end{bmatrix} \tag{22} $$

Preprints (www.preprints.org) | NOT PEER-REVIEWED | Posted: 7 June 2018 doi:10.20944/preprints201806.0111.v1

As it was expected, the solution of the forward acceleration analysis of the HRM is unique while for the inverse acceleration analysis we have an infinite of solutions, a virtue of the redundancy of HRM. On the other hand, by resorting to the theory of helicoidal vector fields it follows that the reduced acceleration state of the ith end-effector taking E_i as the reference pole may obtained as

$$ {}^{0}\boldsymbol{A}_{Ei}^{Ei} = \begin{bmatrix} \boldsymbol{\alpha}_{Ei} \\ \boldsymbol{a}_{Ei} - \boldsymbol{\alpha}_{Ei} \times \boldsymbol{v}_{Ei} \end{bmatrix} = \begin{bmatrix} p({}^{0}\boldsymbol{A}_{G}^{Ei}) \\ d({}^{0}\boldsymbol{A}_{G}^{Ei}) + p({}^{0}\boldsymbol{A}_{G}^{Ei}) \times \boldsymbol{r}_{E_i/G} \end{bmatrix} \tag{23} $$

where $\boldsymbol{\alpha}_{Ei}$ is the angular acceleration vector of the ith end-effector while $\boldsymbol{a}_{Ei}$ is the linear acceleration vector of point E_i.

5. Numerical Example

In order to show the application of the method of kinematic analysis, in this section a case study is provided. In that concern it is interesting to take into account that Huang [9] applied a parametric variation method with the purpose to optimize the dimensions of the 5R mechanism according to the solution of a multi-variable non-linear system generated with the objective to enlarge the workspace and also to alleviate singularities. The optimal parameters of that research for the 5R mechanism was proposed as $a = 1.9$m, $b = 2.1$m, $h = 1.407$m. In the contribution the remaining parameters of the HRM manipulators are chosen as $c = b/2 = 1.05$m, $d = 0.75$m, $r = 0.5$m. There is nothing special in these last parameters.

The first part of the example deals with the forward displacement analysis. With this hope, assume that the generalized coordinates are given by $\underline{q}_1 = 125^o$, $q_1 = 55^o$, $\bar{q}_1 = 280^o$, $\underline{q}_2 = 50^o$, $q_2 = 245^o$, $\bar{q}_2 = 110^o$. After a few computations, the application of the method explained in section 3.2 yields two possible configurations of the HRM which are illustrated in Fig. 4.

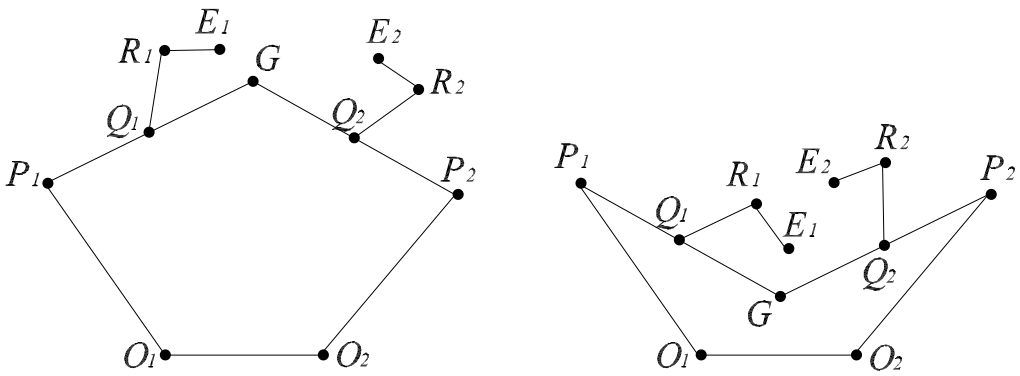

Figure 4. Case study. Available configurations of the hybrid robot manipulator

The next part of the exercise is devoted to the numerical solution of the instantaneous kinematics of the HRM. To this end let us consider that upon the reference configuration, left pose of Fig. 4, the generalized coordinates are commanded to follow periodical functions given by

$$ \begin{aligned} &\underline{q}_1 = 0.15\sin(t), q_1 = 0.25[\sin(t) + \sin(4t) + \sin(2t)\cos(t)], \bar{q}_1 = 0.25\sin(t)\cos(t), \\ &\underline{q}_2 = -0.1\sin(t), q_2 = 0.1[\sin(4t) - \sin(t)], \bar{q}_2 = -0.1\sin(t) \end{aligned} $$

where the time t is given in the interval $0 \leq t \leq 2\pi$. Said otherwise, the period of the generalized coordinates is 2π. The temporal behavior of the kinematics of the end-effectors by applying the proposed method in the contribution is summarized in the plots provided in Fig. 5.

 doi:10.20944/preprints201806.0111.v1

Furthermore, the numerical results shown in Fig. 5 are compared with results obtained using another approach such as special software like ADAMS,™ the corresponding plots are given in Fig. 6.

Finally, it is worth to note that the results obtained by applying the theory of screws are in excellent agreement with those generated with ADAMS.™

6. Conclusions

In this work the kinematics of a hybrid robot manipulator composed of two 2R open kinematic chains sharing a five-bar planar mechanism is approached by means of the theory of screws. The displacement analysis of the HRM is easy to follow owing the fact that closed-form solutions are obtained based on closure equations that lead us simple quadratic equations. After, the instantaneous kinematics of the HRM is carried out by solving firstly the velocity and acceleration analyses of the five-bar planar mechanism. The input-output equations of velocity and acceleration of the five-bar mechanism are systematically obtained by resorting to reciprocal-screw theory. Finally, the velocity and acceleration analyses of the end-effectors are performed by considering that their revolute joints are actuated. A case study is included with the purpose to exemplify the method of kinematic analysis. Furthermore, the numerical results of the instantaneous kinematics of the case study obtained by means of the theory of screws were verified with the aid of commercially available software like ADAMS.™

Acknowledgment

The first author acknowledge with thanks the support of the National Council of Science and Technology of Mexico (CONACYT) through National Network of Researchers (SNI) fellowship. Grant number 7903.

Author Contributions

The displacement analysis of the hybrid robot manipulator was carried out by Ramon Rodriguez-Castro and Luciano Perez-Gonzalez. Jaime Gallardo-Alvarado realized the velocity and acceleration analyses of the HRM as well as the solution of the numerical examples. Carlos R. Aguilar-Najera made the translation of the mathematical framework developed for the kinematics of the HRM into computer codes. Alvaro Sanchez-Rodriguez modeled the HRM in the special software of simulation ADAMS.™ Jaime Gallardo-Alvarado is the first author of the contribution.

Conflicts of Interest

The authors declare no conflict of interest.

1. Hoevenaars, A.G.L.; Gosselin, C.; Lambert, P.; Herder, J.L. A systematic approach for the Jacobian analysis of parallel manipulators with two end-effectors. *Mech. Mach. Theory* **2017**, *109*, 171-194.
2. Balli, S.S.; Chand, S. Synthesis of a five-bar mechanism with variable topology for motion between extreme positions (SYNFBVTM). *Mech. Mach. Theory* **2001**, *36*, 1147-1156.
3. Liu, X.-J.; Wang, J.; Pritschow, G. Kinematics, singularity and workspace of planar 5R symmetrical parallel mechanisms, *Mech. Mech. Theory* **2006**, 41, 145-169.
4. Joubair, A.; Slamani, M.; Bonev, I.A. Kinematic calibration of a five-bar planar parallel robot using all working modes. *Mech. Mach. Theory* **2013**, 29, 15-25.
5. Nafees, K.; Mohammad, A. Synthesis of a planar five-bar mechanism consisting of two binary links having two offset tracing points for motion between two extreme positions. *ASME J. Mech. Robot.* **2016**, *8*, Paper No: JMR-15-1302.
6. Six, D.; Briot, S.; Chriette, A.; Martinet, P. A controller avoiding dynamic model degeneracy of parallel robots during singularity crossing. *ASME J. Mech. Robot.* **2017**, *9*, Paper No: JMR-17-1046.

 doi:10.20944/preprints201806.0111.v1

7. Briot, S.; Goldsztejn, A. Topology optimization of industrial robots: Application to a five-bar mechanism. *Mech. Mach. theory* **2018**, *120*, 30-56.
8. Gallardo-Alvarado, J. *Kinematic Analysis of Parallel Manipulators by Algebraic Screw Theory*. Springer International Publishing, **2016**.
9. Huang, M.Z. Design of a planar parallel robot for optimal workspace and dexterity. *Int. J. Adv. Robot. Sys.* **2011**, *8*, 176-183.

Preprints (www.preprints.org) | NOT PEER-REVIEWED | Posted: 7 June 2018 doi:10.20944/preprints201806.0111.v1

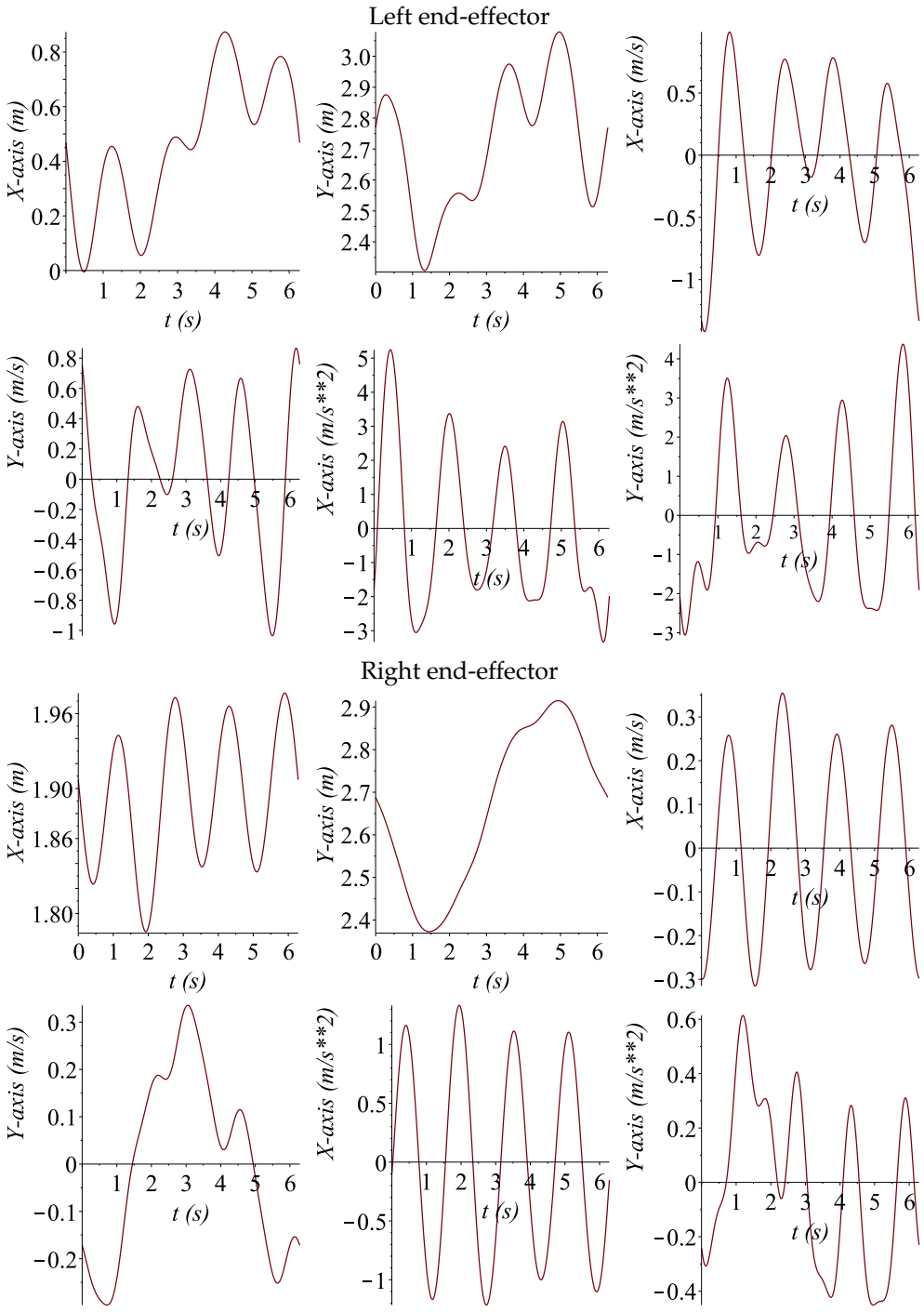

Figure 5. Case study. Instantaneous kinematics of the end-effectors of the hybrid robot manipulator using screw theory

Preprints (www.preprints.org) | NOT PEER-REVIEWED | Posted: 7 June 2018 doi:10.20944/preprints201806.0111.v1

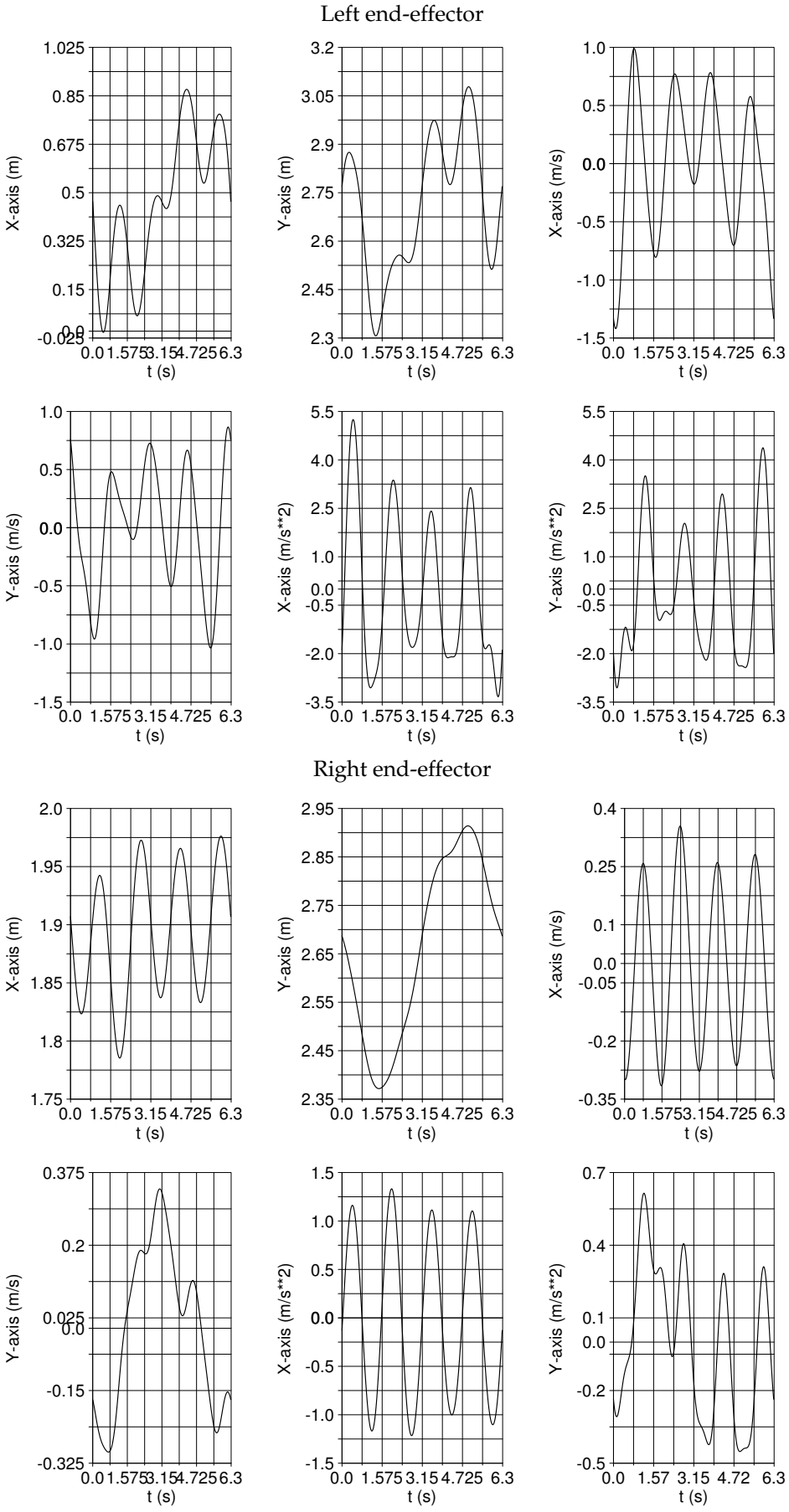

Figure 6. Case study. Instantaneous kinematics of the end-effectors of the hybrid robot manipulator using ADAMS™